

World Journal of *Clinical Cases*

World J Clin Cases 2024 August 26; 12(24): 5448-5635



EDITORIAL

- 5448 Diagnostic challenges from conflicting results of tests and imaging
Yu R
- 5452 Are case reports valuable? Exploring their role in evidence based medicine and patient care
Suvvari TK
- 5456 Recent advances in managing obstructive sleep apnea
Nag DS, Chatterjee A, Patel R, Sen B, Pal BD, Wadhwa G
- 5462 Importance of risk assessment, endoscopic hemostasis, and recent advancements in the management of acute non-variceal upper gastrointestinal bleeding
Maity R, Dhali A, Biswas J
- 5468 Navigating treatment resistance: Janus kinase inhibitors for ulcerative colitis
Soldera J
- 5473 Clues for diagnosing misplaced central venous catheter in the right ascending lumbar vein during right femoral venous access
Tokumine J, Moriyama K, Yorozu T

MINIREVIEWS

- 5476 Exploration of the complex origins of primary constipation
Zeng XL, Zhu LJ, Yang XD

ORIGINAL ARTICLE**Retrospective Study**

- 5483 Influence of humanistic care-based operating room nursing on safety, recovery, and satisfaction after radical surgery for colorectal carcinoma
Wang XP, Niu M
- 5492 Correlation between TEX14 and ADAM17 expressions in colorectal cancer tissues of elderly patients and neoplasm staging, invasion, and metastasis
Chen G, Cong LH, Gu CJ, Li P
- 5502 Assessment of early factors for identification or prediction severe acute pancreatitis in pregnancy
Mei LF, Gan Q, Hu J, Li YX, Tian R, Shi CJ
- 5513 Application value of machine learning models in predicting intraoperative hypothermia in laparoscopic surgery for polytrauma patients
Zhu K, Zhang ZX, Zhang M

Clinical Trials Study

- 5523 Effectiveness of the A3 robot on lower extremity motor function in stroke patients: A prospective, randomized controlled trial

Zhang LJ, Wen X, Peng Y, Hu W, Liao H, Liu ZC, Liu HY

- 5534 Effect of dietary with Zhibai dihuang pills and gonadotropin-releasing-hormone-analogue on girls with precocious and rapidly progressive puberty

Wang XM, Li W, Yang LQ, Luo R, Zhang CC

Randomized Controlled Trial

- 5542 Clinical efficacy, bone density, and follow-up in implant and orthodontic treatment for inclined adjacent teeth

Yang Y, Zhou SC, Ma YH, Wang X, Dong QS

- 5549 Information-motivation-behavioral guided nursing for stroke patients with pulmonary dysfunction: A randomized controlled trial

Peng X, Ni HQ, Liu YM, Zhu JL, Bai YT

- 5558 Application of buried auricular point combined with Wenjing Sanhan prescription in arteriosclerosis obliterans patients with resting pain

Li YP, Su T, Xue XL, Shi HR, Su ZH, Li J

Clinical and Translational Research

- 5568 Computed tomography-based radiomics predicts the fibroblast-related gene *EZH2* expression level and survival of hepatocellular carcinoma

Yu TY, Zhan ZJ, Lin Q, Huang ZH

CASE REPORT

- 5583 Endometrial carcinoma with cervical stromal invasion: Three case reports

Liu MM, Liang YT, Jin EH

- 5589 IgG4-related sclerosing cholangitis associated with essential thrombocythemia: A case report

Wu ZN, Ji R, Xiao Y, Wang YD, Zhao CY

- 5596 Are all primary omental infarcts truly idiopathic? Five case reports

Kar H, Khabbazazar D, Acar N, Karasu Ş, Bağ H, Cengiz F, Dilek ON

- 5604 Seven-years post allogeneic hematopoietic stem cell transplantation pure red cell aplastic anemia cured with daratumumab: A case report and review of literature

Deng B, Gao R, Yang B, Lei WB, Xue MF, Wang JS, Zhao P

- 5613 Splenic subcapsular hematoma following endoscopic retrograde cholangiopancreatography: A case report and review of literature

Guo CY, Wei YX

- 5622** "Keyboard sign" and "coffee bean sign" in the prenatal diagnosis of ileal atresia: A case report
Fei ZH, Zhou QY, Fan L, Yin C
- 5628** Treatment of nasopharyngeal carcinoma and prevention of non-alcoholic Wernicke's disease: A case report and review of literature
Ma YY, He XC, Gao Y, Ma TT, Cheng G, Yue CW

ABOUT COVER

Peer Reviewer of *World Journal of Clinical Cases*, Madhukar Mittal, FACE, MBBS, MD, Professor, Endocrinology and Metabolism, All India Institute of Medical Sciences Jodhpur, Jodhpur 342005, India. mittalspace@gmail.com

AIMS AND SCOPE

The primary aim of *World Journal of Clinical Cases* (*WJCC*, *World J Clin Cases*) is to provide scholars and readers from various fields of clinical medicine with a platform to publish high-quality clinical research articles and communicate their research findings online.

WJCC mainly publishes articles reporting research results and findings obtained in the field of clinical medicine and covering a wide range of topics, including case control studies, retrospective cohort studies, retrospective studies, clinical trials studies, observational studies, prospective studies, randomized controlled trials, randomized clinical trials, systematic reviews, meta-analysis, and case reports.

INDEXING/ABSTRACTING

The *WJCC* is now abstracted and indexed in Science Citation Index Expanded (SCIE, also known as SciSearch®), Journal Citation Reports/Science Edition, Current Contents®/Clinical Medicine, PubMed, PubMed Central, Reference Citation Analysis, China Science and Technology Journal Database, and Superstar Journals Database. The 2024 Edition of Journal Citation Reports® cites the 2023 journal impact factor (JIF) for *WJCC* as 1.0; JIF without journal self cites: 0.9; 5-year JIF: 1.1; JIF Rank: 168/325 in medicine, general and internal; JIF Quartile: Q3; and 5-year JIF Quartile: Q3.

RESPONSIBLE EDITORS FOR THIS ISSUE

Production Editor: Zi-Hang Xu, Production Department Director: Xu Guo, Cover Editor: Jin-Lai Wang.

NAME OF JOURNAL

World Journal of Clinical Cases

ISSN

ISSN 2307-8960 (online)

LAUNCH DATE

April 16, 2013

FREQUENCY

Thrice Monthly

EDITORS-IN-CHIEF

Bao-Gan Peng, Salim Surani, Jerzy Tadeusz Chudek, George Kontogeorgos, Maurizio Serati

EDITORIAL BOARD MEMBERS

<https://www.wjgnet.com/2307-8960/editorialboard.htm>

PUBLICATION DATE

August 26, 2024

COPYRIGHT

© 2024 Baishideng Publishing Group Inc

INSTRUCTIONS TO AUTHORS

<https://www.wjgnet.com/bpg/gerinfo/204>

GUIDELINES FOR ETHICS DOCUMENTS

<https://www.wjgnet.com/bpg/GerInfo/287>

GUIDELINES FOR NON-NATIVE SPEAKERS OF ENGLISH

<https://www.wjgnet.com/bpg/gerinfo/240>

PUBLICATION ETHICS

<https://www.wjgnet.com/bpg/GerInfo/288>

PUBLICATION MISCONDUCT

<https://www.wjgnet.com/bpg/gerinfo/208>

ARTICLE PROCESSING CHARGE

<https://www.wjgnet.com/bpg/gerinfo/242>

STEPS FOR SUBMITTING MANUSCRIPTS

<https://www.wjgnet.com/bpg/GerInfo/239>

ONLINE SUBMISSION

<https://www.f6publishing.com>

Clinical and Translational Research

Computed tomography-based radiomics predicts the fibroblast-related gene *EZH2* expression level and survival of hepatocellular carcinoma

Ting-Yu Yu, Ze-Juan Zhan, Qi Lin, Zhen-Huan Huang

Specialty type: Medicine, research and experimental**Provenance and peer review:** Unsolicited article; Externally peer reviewed.**Peer-review model:** Single blind**Peer-review report's classification****Scientific Quality:** Grade C**Novelty:** Grade C**Creativity or Innovation:** Grade C**Scientific Significance:** Grade C**P-Reviewer:** Tai DI, Taiwan**Received:** April 9, 2024**Revised:** May 21, 2024**Accepted:** June 12, 2024**Published online:** August 26, 2024**Processing time:** 93 Days and 1 Hours**Ting-Yu Yu, Ze-Juan Zhan, Qi Lin, Zhen-Huan Huang**, Department of Radiology, Longyan First Affiliated Hospital of Fujian Medical University, Longyan 364000, Fujian Province, China**Co-first authors:** Ting-Yu Yu and Ze-Juan Zhan.**Corresponding author:** Zhen-Huan Huang, MD, Associate Chief Physician, Department of Radiology, Longyan First Affiliated Hospital of Fujian Medical University, No. 105 Jiu Yi North Road, Xin Luo District, Longyan 364000, Fujian Province, China. tuxuezhao@163.com

Abstract

BACKGROUND

Hepatocellular carcinoma (HCC) is the most common subtype of liver cancer. The primary treatment strategies for HCC currently include liver transplantation and surgical resection. However, these methods often yield unsatisfactory outcomes, leading to a poor prognosis for many patients. This underscores the urgent need to identify and evaluate novel therapeutic targets that can improve the prognosis and survival rate of HCC patients.

AIM

To construct a radiomics model that can accurately predict the *EZH2* expression in HCC.

METHODS

Gene expression, clinical parameters, HCC-related radiomics, and fibroblast-related genes were acquired from public databases. A gene model was developed, and its clinical efficacy was assessed statistically. Drug sensitivity analysis was conducted with identified hub genes. Radiomics features were extracted and machine learning algorithms were employed to generate a radiomics model related to the hub genes. A nomogram was used to illustrate the prognostic significance of the computed Radscore and the hub genes in the context of HCC patient outcomes.

RESULTS

EZH2 and *NRAS* were independent predictors for prognosis of HCC and were utilized to construct a predictive gene model. This model demonstrated robust performance in diagnosing HCC and predicted an unfavorable prognosis. A

negative correlation was observed between *EZH2* expression and drug sensitivity. Elevated *EZH2* expression was linked to poorer prognosis, and its diagnostic value in HCC surpassed that of the risk model. A radiomics model, developed using a logistic algorithm, also showed superior efficiency in predicting *EZH2* expression. The Radscore was higher in the group with high *EZH2* expression. A nomogram was constructed to visually demonstrate the significant roles of the radiomics model and *EZH2* expression in predicting the overall survival of HCC patients.

CONCLUSION

EZH2 plays significant roles in diagnosing HCC and therapeutic efficacy. A radiomics model, developed using a logistic algorithm, efficiently predicted *EZH2* expression and exhibited strong correlation with HCC prognosis.

Key Words: Hepatocellular carcinoma; Fibroblast; *EZH2*; Radiomics model; Diagnosis; Prognosis

©The Author(s) 2024. Published by Baishideng Publishing Group Inc. All rights reserved.

Core Tip: This study integrated radiomics molecular analysis based on computed tomography images. It aimed to identify important molecular biomarkers associated with hepatocellular carcinoma (HCC), particularly *EZH2*, and establish a radiomics model to predict *EZH2* expression and its association with the prognosis of HCC patients. The results of this study demonstrated a close correlation between the radiomics model, *EZH2* expression, and HCC patient prognosis, suggesting that a radiomics analysis can provide additional molecular information and offer a new approach to clinical treatment of HCC.

Citation: Yu TY, Zhan ZJ, Lin Q, Huang ZH. Computed tomography-based radiomics predicts the fibroblast-related gene *EZH2* expression level and survival of hepatocellular carcinoma. *World J Clin Cases* 2024; 12(24): 5568-5582

URL: <https://www.wjgnet.com/2307-8960/full/v12/i24/5568.htm>

DOI: <https://dx.doi.org/10.12998/wjcc.v12.i24.5568>

INTRODUCTION

Liver cancer, a highly heterogeneous and malignant tumor associated with the digestive system, is the fourth-leading cause of cancer-related fatalities worldwide[1,2]. Hepatocellular carcinoma (HCC), the most common subtype of liver cancer, accounts for over 75% of all cases[3]. In China, HCC is responsible for the second-highest cancer mortality rate. This is due to various factors including historical, demographic, and health conditions[4]. Major contributors to the development of HCC include chronic infection with hepatitis B virus or hepatitis C virus, excessive alcohol consumption, and liver fibrosis[5]. Presently, the major treatment strategies for HCC are liver transplantation and surgical resection, but these methods often yield unsatisfactory outcomes[6]. This underscores the urgent need to identify novel therapeutic targets that can improve the prognosis and overall survival (OS) rate of HCC patients.

Persistent liver damage and fibrosis are significant risk factors for HCC development[7]. Research indicates that most HCC patients had preexisting cirrhosis, with approximately one-third of these cirrhosis patients eventually developing HCC[8]. Moreover, the tumor microenvironment (TME) has been shown to facilitate tumor progression[9]. In HCC, the interactions within the TME, composed of cancer-associated fibroblasts (CAFs), immune cells, endothelial cells, and HCC cells, significantly increase tumor proliferation, invasion, metastasis, and chemoresistance[9]. Additionally, CAFs, the primary component in TME stroma, have previously been shown to promote the aggressiveness of various cancers, including HCC[10,11].

Genetics plays a crucial role in understanding the structure and function of organisms and has been widely applied in various medical fields, including clinical diagnosis, drug development, and disease prediction. In this study, an enhancer of the *EZH2* subunit was identified as a key fibroblast-related gene (FRG) in HCC. Furthermore, *EZH2* demonstrated significant diagnostic value in HCC. As a core component of the polycomb repressive complex 2, *EZH2* is involved in the onset and progression of various cancers, including prostate, breast, melanoma, bladder, and endometrial[12]. In malignant tumors, *EZH2* suppresses the expression of numerous tumor suppressor genes, thereby facilitating carcinogenesis[13].

Radiomics, an emerging technological tool, transforms standard medical images into quantitative representations. By analyzing quantitative imaging features, radiomics has substantially lowered the cost of diagnosing diseases and the need for invasive surgeries[14]. Preoperative computed tomography (CT) radiomics is widely used for diagnosing, staging, and assessing the treatment efficacy in HCC, demonstrating robust evaluation and prediction capabilities[15].

In this study, FRGs were retrieved and used to develop a gene model associated with HCC prognosis through various bioinformatics analyses. The drug sensitivity analysis and molecular docking results highlighted the significant role of *EZH2* in treating HCC patients. Subsequently, leveraging CT images, this study aimed to establish a radiomics model for predicting *EZH2* expression levels, offering valuable insights for clinical HCC treatment.

MATERIALS AND METHODS

RNA-seq and CT imaging data collection

Figure 1 illustrates the research process undertaken in this study. RNA-seq data and clinicopathological information (age, sex, pathological stage, and grade) of HCC patients were retrieved from The Cancer Genome Atlas (TCGA) database (<https://tcga-data.nci.nih.gov/tcga/>). The samples without complete expression and clinical information in the TCGA-HCC dataset were excluded. Subsequently, HCC patient CT image data was downloaded from The Cancer Imaging Archive (TCIA) database (<http://www.cancerimagingarchive.net>). The TCIA data was carefully filtered to exclude any data that did not overlap with the TCGA data as well as CT images from tumor excision patients and those with poor image pixels. Ultimately, this study included 339 HCC tumor samples, 50 normal samples, and 41 imaging datasets. Notably, all tumor samples received radiation and pharmaceutical therapy. Additionally, the GSE25097 dataset, comprising 249 normal and 268 HCC samples, was retrieved from the Gene Expression Omnibus database, using the GPL10687 platform.

Acquisition and enrichment analysis of differentially expressed FRG in HCC

The GeneCard database (<https://www.genecards.org/>) was used to screen for FRGs, using the keyword “Fibroblast.” Next, differentially expressed genes (DEGs) between normal and tumor tissues in the TCGA-HCC dataset were identified using the limma package in R language, with a threshold setting of $|\log_2(\text{Fold change})| > 2.0$ and $P < 0.05$. Finally, Venn diagram analysis was used to identify FRGs that are DEGs in HCC.

Gene Ontology (GO) and Kyoto Encyclopedia of Genes and Genomes (KEGG) enrichment analyses were conducted on the FRGs differentially expressed in HCC, using the org.Hs.eg.db and clusterProfiler packages in R software. GO describes the function of all gene products in various organisms and identifies characteristic biological features of high-throughput genomes, including biological process, cellular component, and molecular function[16]. KEGG is a widely used database that stores information on genomes, biological pathways, diseases, and drugs.

Construction of a gene model

Firstly, least absolute shrinkage and selection operator regression analysis was performed on the differentially expressed FRGs using the glmnet package in R software to identify key genes associated with the OS of HCC patients from the TCGA dataset. Secondly, univariate and multivariate Cox regression analyses were conducted sequentially to identify genes significantly associated with HCC prognosis. Finally, based on the multivariate Cox regression analysis, an HCC prognostic gene model was established using the following formula: Risk score = gene $\exp_1 \times \beta_1 + \text{gene } \exp_2 \times \beta_2 + \dots + \text{gene } \exp_n \times \beta_n$, where “gene exp” represents the expression level of the gene, and β represents the corresponding coefficient of the multivariate Cox regression.

Evaluation and validation of the gene model

The receiver operating characteristic (ROC) curve analysis was performed on the TCGA and GSE25097 HCC datasets using the R package pROC. This was to assess the diagnostic efficacy of the gene model. Kaplan-Meier analysis of the risk score and OS in the TCGA data was conducted using the survival package and visualized using the survminer package in R software. Additionally, R software generated a forest plot to determine the relationship between the gene risk score and HCC prognosis across different clinical feature groups. Multivariate Cox regression analysis was employed to verify the independent prognostic value of the risk score.

Drug sensitivity analysis and molecular docking

The Cancer Therapeutics Response Portal database contains data on the sensitivity of different tumor cells to various chemotherapy drugs. The database was used to calculate the sensitivity of genes to different chemotherapy drugs with the help of the oncoprdict package in R software. Then, the crystal structures of these genes were obtained from the Research Collaboratory for Structural Bioinformatics database (<https://www.rcsb>). The binding efficiency of genes with crucial chemotherapy drugs was analyzed using the Autodock software (Version 4.2.6). A binding energy $l \leq -1.5$ kcal/mol indicates a good binding effect[17].

Extraction of radiomics features

The entire tumor region was manually delineated by two radiologists using 3D Slicer (Version 5.4.0) who also independently described the lesions without knowledge of the patient’s clinical details. The pyradiomics package in Python software was used for radiomics feature extraction and data normalization. A total of 837 radiomics features were acquired, including first-order features, shape, and texture.

The intraclass correlation coefficient was calculated using the R “irr” package to evaluate the consistency of the extracted radiomics features based on the region of interest outlined by the two radiologists. Intraclass correlation coefficient values ≥ 0.75 indicated good consistency, 0.51-0.74 indicated moderate consistency, and ≤ 0.50 indicated poor consistency[18].

Selection of radiomics features

The TCIA image data related to HCC were divided into two groups based on the median expression level of *EZH2*. Radiomics features related to *EZH2* were selected using the XG Boost package in Python. Feature importance analysis was conducted using multiple machine learning algorithms to identify radiomics features closely associated with *EZH2*.

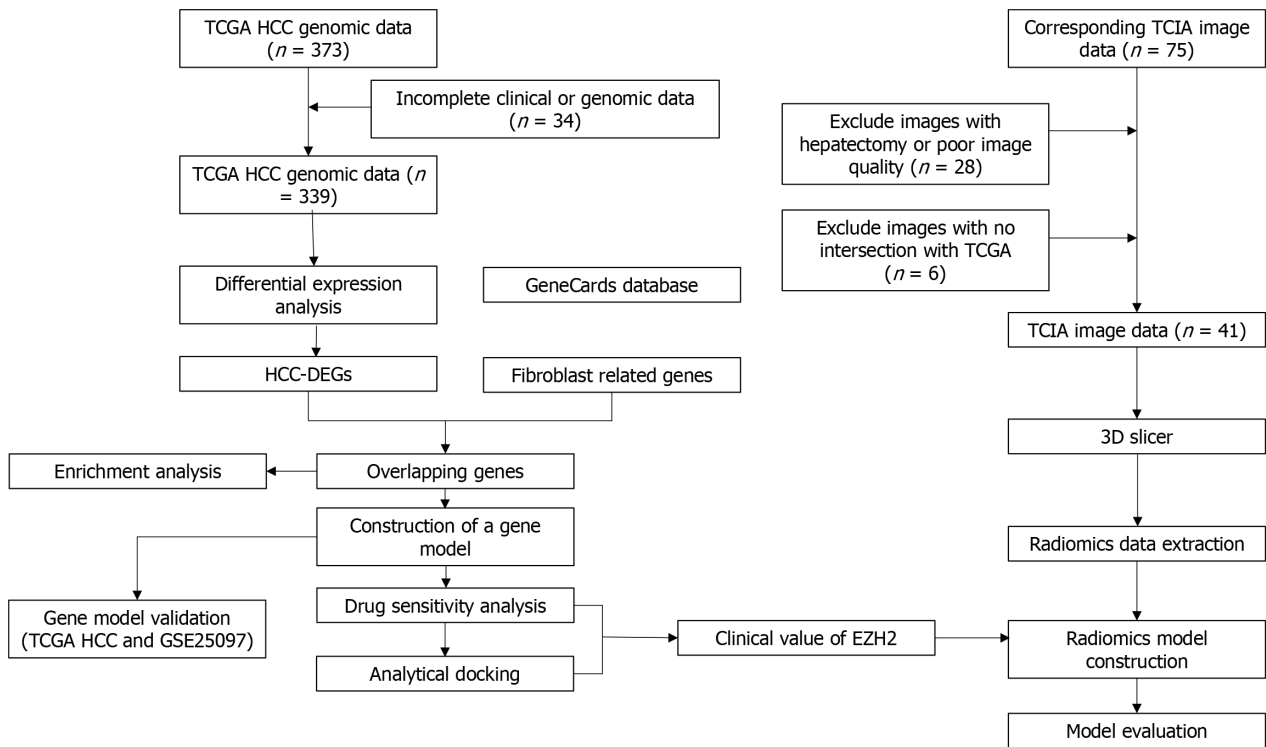


Figure 1 Entire analytical process of the study. DEGs: Differentially expressed genes; HCC: Hepatocellular carcinoma; TCGA: The Cancer Genome Atlas; TCIA: The Cancer Imaging Archive.

Construction and evaluation of the radiomics model

Two radiomics models related to *EZH2*, specifically logistic regression and random forest models, were constructed using multiple machine learning algorithms. A comprehensive multimodel analysis was conducted to determine the radiomics model with superior performance in predicting *EZH2*. Subsequently, a restricted cubic spline analysis was executed on the Radscore and *EZH2* using the rms package in R software to predict their nonlinear relationship. Ultimately, a nomogram was constructed to evaluate the correlation of *EZH2* and Radscore and the prognosis of HCC patients.

Statistical analysis

Data analysis and visualization were performed using R (Version 4.2.2) and Python (Version 3.6.6). Quantitative data was expressed as mean \pm standard deviation, median, or quartile. The Student's *t*-test or Wilcoxon test was employed to analyze comparisons between groups. Categorical variables were represented as counts and percentages, and group comparisons were performed using the χ^2 test. The Delong test was used to compare the differences in area under the curve (AUC) values. A *P* value of less than 0.05 was considered statistically significant.

RESULTS

Identification and enrichment analysis of differentially expressed FRGs

Initially, 144247 FRGs were extracted from the GeneCards database, but this was narrowed down to 666 FRGs based on a threshold score ≥ 5 . A differential analysis of the HCC data revealed 8205 DEGs between HCC and normal tissues, which included 7366 upregulated genes and 839 downregulated genes ($P < 0.05$, Figure 2A). A total of 299 FRGs were identified to be differentially expressed in HCC (Figure 2B).

The biological processes that differentially expressed FRGs are a part of were identified by enrichment analysis in GO. The analysis revealed that these genes were primarily a part of various stimuli response pathways, such as chemicals, organic substances, and stress. Some were also involved in cell proliferation (Figure 2C). KEGG enrichment analysis revealed that the differentially expressed FRGs were primarily associated with pathways known to play a role in cancer pathogenesis and survival, such as PI3K-Akt signaling pathway, proteoglycans in cancer, focal adhesion, hepatitis B, HCC, and hepatitis C alcoholism (Figure 2D). These pathways are closely related to the onset and development of tumors.

Construction of a gene model

To construct a gene model associated with HCC prognosis, a sequence of analyses was conducted, including least absolute shrinkage and selection operator regression analysis as well as univariate and multivariate Cox regression. Among the 299 differentially expressed FRGs, 7 genes were significantly associated with the OS of HCC patients

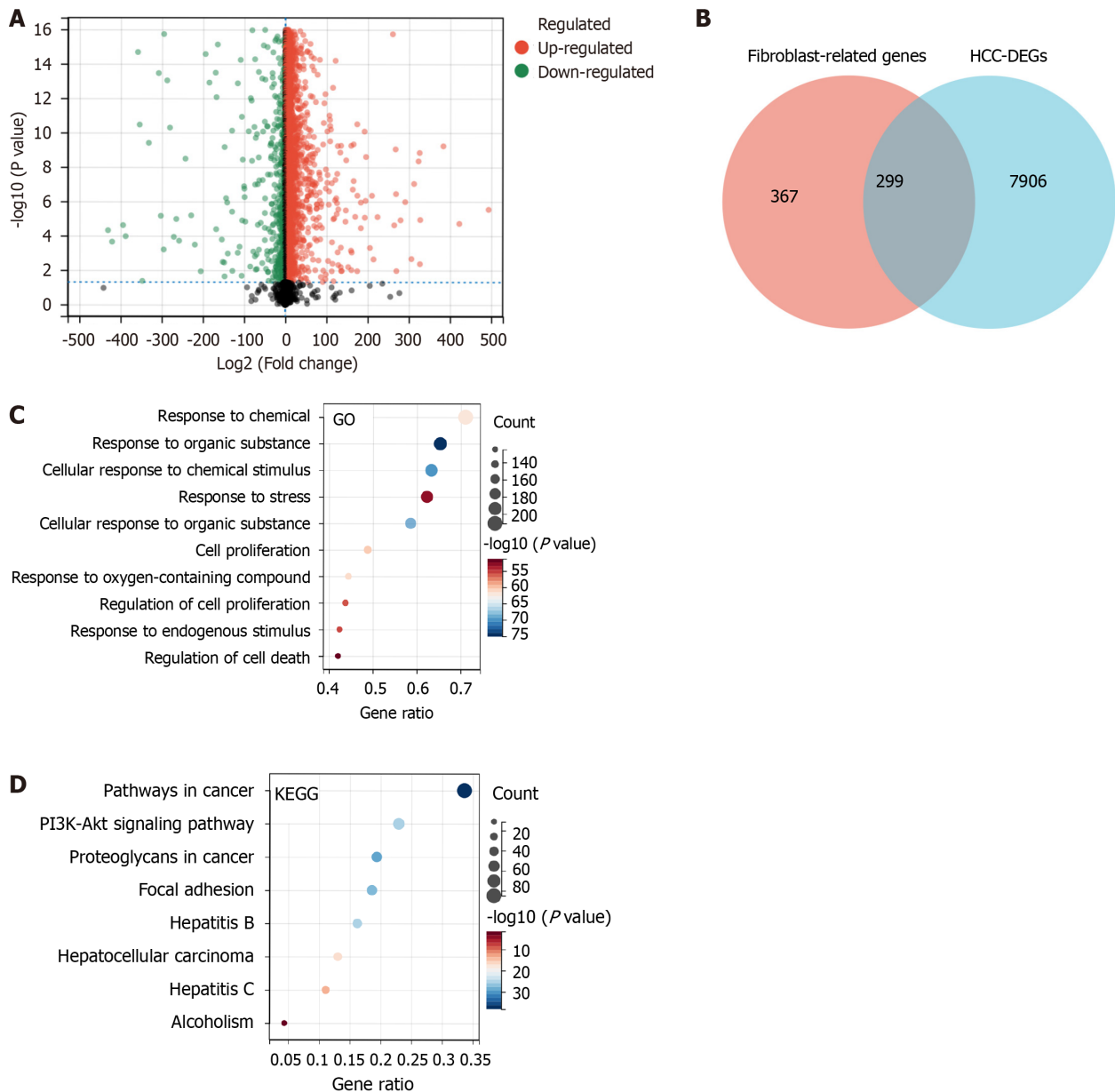


Figure 2 Identification and enrichment analysis of differentially expressed fibroblast-related genes. A: Volcano plot was used to visualize the results of differential analysis between normal and tumor tissues in hepatocellular carcinoma (HCC); B: Venn diagram of fibroblast-related genes (FRGs) and HCC-differentially expressed genes (DEGs); C: Gene ontology (GO) enrichment analyses of differentially expressed FRGs; D: Kyoto Encyclopedia of Genes and Genomes (KEGG) enrichment analyses of differentially expressed FRGs.

(Figure 3). Furthermore, *EZH2* and *NRAS* were found to independently predict the prognosis of HCC patients ($P < 0.05$, Table 1). The gene model was constructed based on the outcomes of the multivariate Cox regression analysis using the formula: Risk score = $0.083 \times EZH2 + 0.03 \times NRAS$.

Evaluation and validation of the gene model

The differential expression analysis of the risk score between the HCC and normal groups was conducted. Notably, significantly higher risk scores were observed in the HCC group in the TCGA and GSE25097 HCC datasets ($P < 0.05$, Figure 4A and B). Additionally, the risk score as a continuous and categorical variable was found to be independent of age, sex, grade, and pathological stage (S1 + S2; stage I and stage II; S3 + S4; stage III and stage IV) ($P > 0.05$, Table 2 and Figure 4C-F). Subsequently, ROC analysis was performed to explore the diagnostic efficiency of the gene model. In the TCGA-HCC and GSE25097 datasets, the gene model efficiently distinguished HCC from normal samples, with an AUC value of 0.94 and 0.95, respectively ($P < 0.05$) (Figure 4G and H). These results indicated that the risk model was highly effective in diagnosing HCC.

Prognostic value of the gene model

A Kaplan-Meier analysis was conducted to investigate the association of the risk score with HCC prognosis. As depicted in Figure 5A, a higher risk score indicates a poor prognosis for HCC patients. Additionally, among HCC patients aged \leq

Table 1 Correlation between key genes and prognosis of hepatocellular carcinoma patients

Characteristic	Total, <i>n</i>	Univariate analysis		Multivariate analysis	
		Hazard ratio (95%CI)	<i>P</i> value	Hazard ratio (95%CI)	<i>P</i> value
<i>ATIC</i>	339	1.042 (1.027-1.058)	< 0.001	1.011 (0.989-1.033)	0.348
<i>EZH2</i>	339	1.196 (1.128-1.269)	< 0.001	1.087 (1.006-1.174)	0.035
<i>HDGF</i>	339	1.010 (1.006-1.014)	< 0.001	1.004 (0.999-1.026)	0.104
<i>HEXB</i>	339	1.027 (1.014-1.039)	< 0.001	1.013 (0.999-1.026)	0.060
<i>HSPA4</i>	339	1.040 (1.023-1.058)	< 0.001	1.017 (0.996-1.039)	0.117
<i>NRAS</i>	339	1.066 (1.042-1.091)	< 0.001	1.031 (1.003-1.059)	0.032
<i>PPT1</i>	339	1.030 (1.019-1.041)	< 0.001	1.004 (0.988-1.020)	0.665

CI: Confidence interval.

Table 2 Relationship between risk score and clinicopathological parameters in hepatocellular carcinoma patients

Variables	Total, <i>n</i> = 339	Risk score-low, <i>n</i> = 170	Risk score-high, <i>n</i> = 169	<i>P</i> value
Age	61.000 (51.000, 68.000)	62.000 (52.000, 69.000)	59.000 (51.000, 67.000)	0.083
Sex				0.310
Female	107 (31.6%)	58 (34.1%)	49 (29.0%)	
Male	232 (68.4%)	112 (65.9%)	112 (71.0%)	
Stage				0.876
S1+S2	252 (74.3%)	127 (74.7%)	125 (74.0%)	
S3+S4	87 (25.7%)	43 (25.3%)	44 (26.0%)	
Grade				0.457
G1+G2	212 (62.5%)	103 (60.6%)	109 (64.5%)	
G3+G4	127 (35.5%)	67 (39.4%)	60 (35.5%)	

S1 + S2: Stage I and stage II; S3 + S4: Stage III and stage IV.

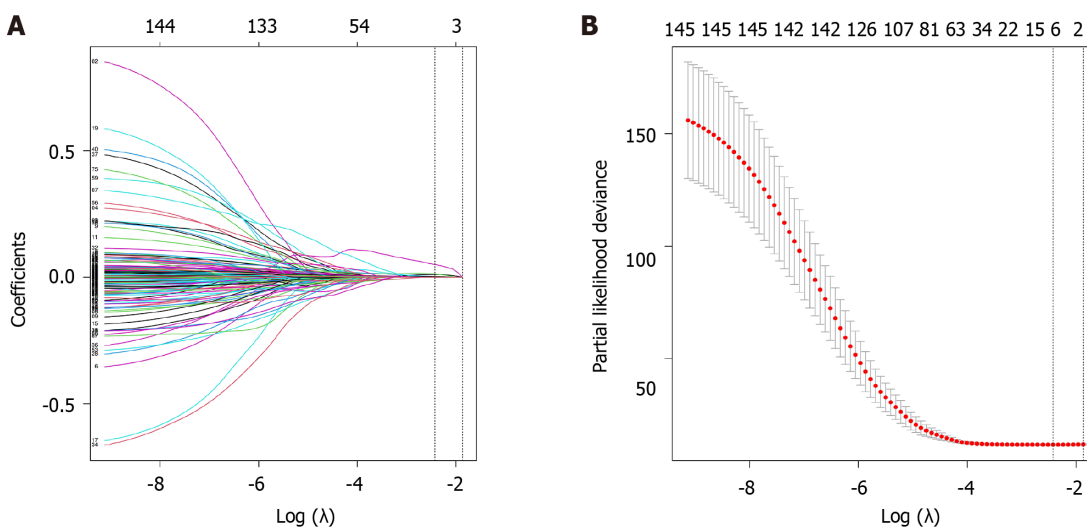


Figure 3 Selection of hub genes related to hepatocellular carcinoma prognosis. A: Least absolute shrinkage and selection operator (LASSO) correlation coefficient change curve; B: LASSO cross-validation curve.

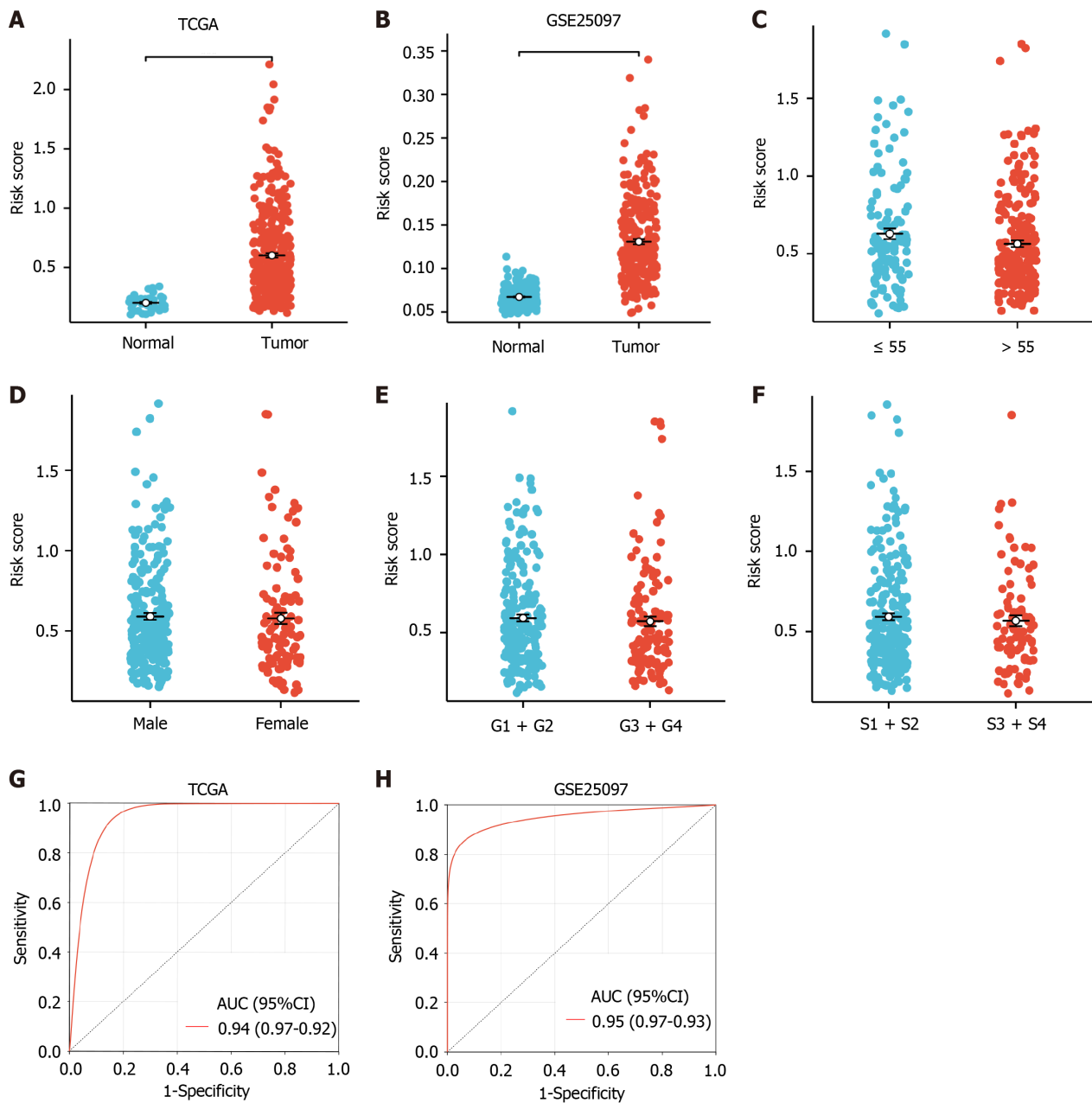


Figure 4 Evaluation and validation of risk model. A and B: Based on the Cancer Genome Atlas (TCGA)-Hepatocellular carcinoma (HCC) and GSE25097 datasets, the risk score was higher in the HCC samples; C: Relationship of risk score with age; D: Relationship of risk score with sex; E: Relationship of risk score with grade; F: Relationship of risk score with pathological stage; G: Receiver operating characteristic (ROC) curve of the risk score in the TCGA-HCC; H: ROC curve of the risk score in the GSE25097 datasets for distinguishing HCC and normal samples. S1 + S2: Stage I and stage II; S3 + S4: Stage III and stage IV. AUC: Area under the curve; CI: Confidence interval.

55 [hazard ratio (HR) = 4.46 (2.32-8.58), $P < 0.05$] and > 55 [HR = 2.55 (1.60-4.07), $P < 0.05$], female [HR = 2.97 (1.25-7.08), $P < 0.05$] and male [HR = 3.03 (1.89-4.85), $P < 0.05$], G1 + G2 [HR = 2.13 (1.36-3.35), $P < 0.05$] and G3 + G4 [HR = 4.15 (2.13-8.09), $P < 0.05$], and S1 + S2 [HR = 3.01 (1.94-4.66), $P < 0.05$] and S3 + S4 [HR = 3.62 (1.63-8.05), $P < 0.05$], high-risk scores were associated with poorer prognosis (Figure 5B). These results indicated that higher risk scores were significantly related to unfavorable prognosis regardless of age, sex, grade, and stage. Furthermore, when age, sex, grade, pathological stage, and risk score were analyzed using a multivariate Cox regression analysis, the results showed that the risk score independently predicted poor prognosis in HCC patients ($P < 0.05$) (Table 3).

Drug sensitivity analysis and molecular docking

The goal was to investigate the therapeutic significance of specific genes within the gene model and identify potential therapeutic targets. To achieve this, the correlation between the expression levels of two genes, *EZH2* and *NRAS*, and the sensitivity of commonly used chemotherapy and targeted drugs were examined. Leveraging data from the Cancer Therapeutics Response Portal database, it was found that *EZH2* expression was significantly negatively correlated with drug sensitivity (Figure 6A). Subsequently, four drugs, belinostat, BRD-K34222889, ciclopirox, and cytarabine hydrochloride, were selected for molecular docking analysis. Remarkably, *EZH2* exhibited favorable interactions with

Table 3 Correlation between risk scores in clinical features and hepatocellular carcinoma prognosis

Characteristic	Total, <i>n</i>	Multivariate analysis	
		Hazard ratio (95%CI)	<i>P</i> value
Risk score	339	5.339 (3.139-9.078)	< 0.001
Age	339	1.018 (1.002-1.034)	0.028
Sex	339	1.010 (1.006-1.014)	0.172
Grade	339	1.113 (0.744-1.664)	0.603
Stage	339	0.888 (0.579-1.363)	0.588

CI: Confidence interval.

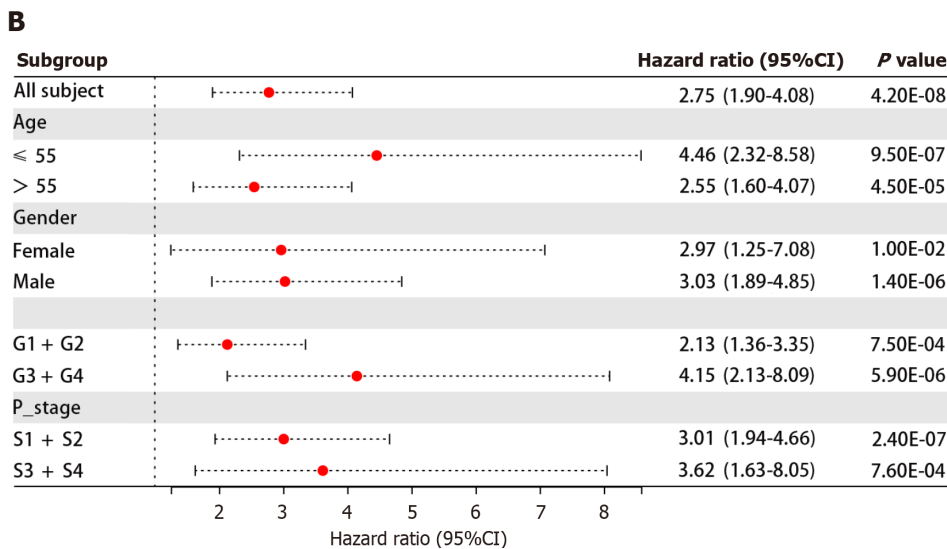
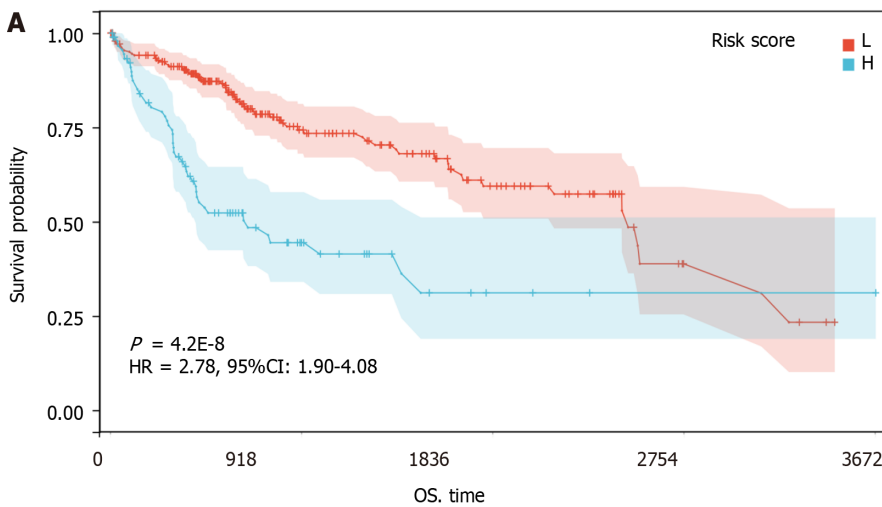


Figure 5 Prognostic model of the risk model. A: Kaplan-Meier curve showed that a higher risk score was associated with poor prognosis; B: Correlation between risk scores in clinical features and hepatocellular carcinoma prognosis. S1 + S2: Stage I and stage II; S3 + S4: Stage III and stage IV. CI: Confidence interval; H: High; HR: Hazard ratio; L: Low; OS: Overall survival.

these drugs (Table 4). The most promising docking outcomes were visualized using the PyMOL software ($P < 0.05$, Figure 6B). These findings underscored the potential of EZH2 as a therapeutic target for HCC, prompting further investigation of its value in HCC treatment.

Clinical value of EZH2 in HCC

The EZH2 protein levels were significantly higher in the HCC group compared to the normal group ($P < 0.05$, Figure 7A). Interestingly, patients with EZH2 overexpression had significantly shorter survival ($P < 0.05$, Figure 7B). Furthermore,

Table 4 Binding energy between EZH2 and four chemotherapy drugs in molecular docking

Medicine	Hub targets (PDB ID)	Binding energy in kcal/mol
Belinostat	EZH2 (5h14)	-4.58
BRD-K34222889	EZH2 (5h14)	-4.23
Ciclopirox	EZH2 (5h14)	-4.07
Cytarabine hydrochloride	EZH2 (5h14)	-1.75

PDB ID: Protein database ID.

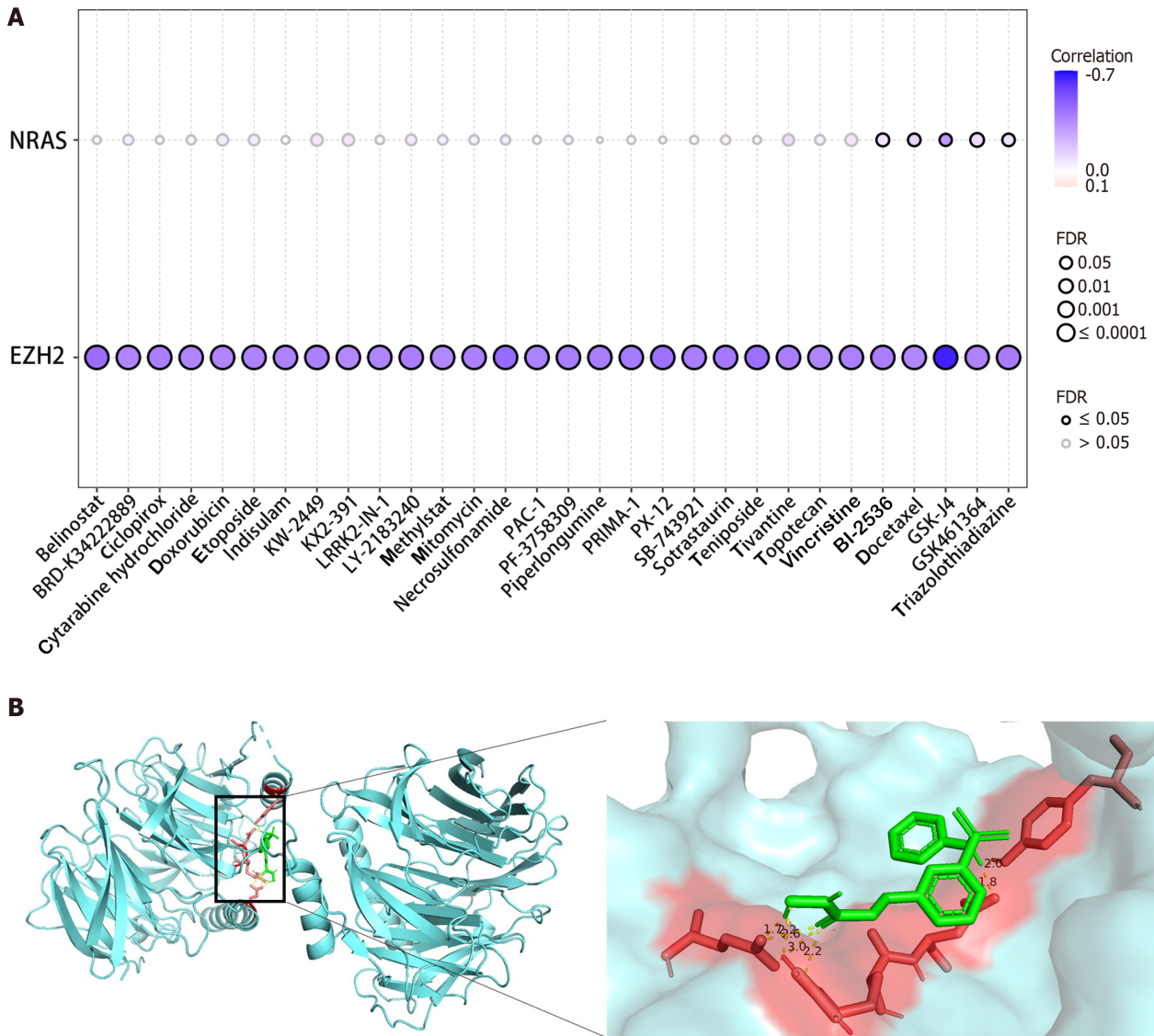


Figure 6 Drug sensitivity analysis and molecular docking. A: Correlation of EZH2 and NRAS with chemotherapy and cancer drugs; B: Molecular docking between EZH2 and belinostat. FDR: False discovery rate.

using the ROC analysis with AUC values, it was shown that EZH2 outperformed NRAS and the risk score in predicting HCC, achieving the highest AUC value of 0.978 ($P < 0.05$, Figure 7C and Table 5). The clinical efficacy of EZH2, NRAS, and the risk score was compared using the decision curve analysis (Figure 7D). These results confirmed the significance of EZH2 in HCC and its potential as a diagnostic marker.

Screening of radiomics features related to EZH2 and radiomics model construction

The XGBoost-RFE algorithm was used to screen the radiomics features related to EZH2. The six features included original_glrIm_LongRunLowGrayLevelEmphasis, original_glrIm-SizeZoneNonUniformityNormalized, wavelet-LHL_glcm-DifferenceAverage, wavelet-LHL_glcm-lmc2, wavelet-LHL_firstorder- Maximum, and wavelet-LHL_glrIm-

Table 5 Difference in the area under the curves of *EZH2*, *NRAS*, and the risk score in diagnosing hepatocellular carcinoma

Name	<i>EZH2</i>	<i>NRAS</i>	Risk score
<i>EZH2</i>	/	< 0.05	< 0.05
<i>NRAS</i>	< 0.05	/	< 0.05
Risk score	< 0.05	< 0.05	/

/: Not applicable.

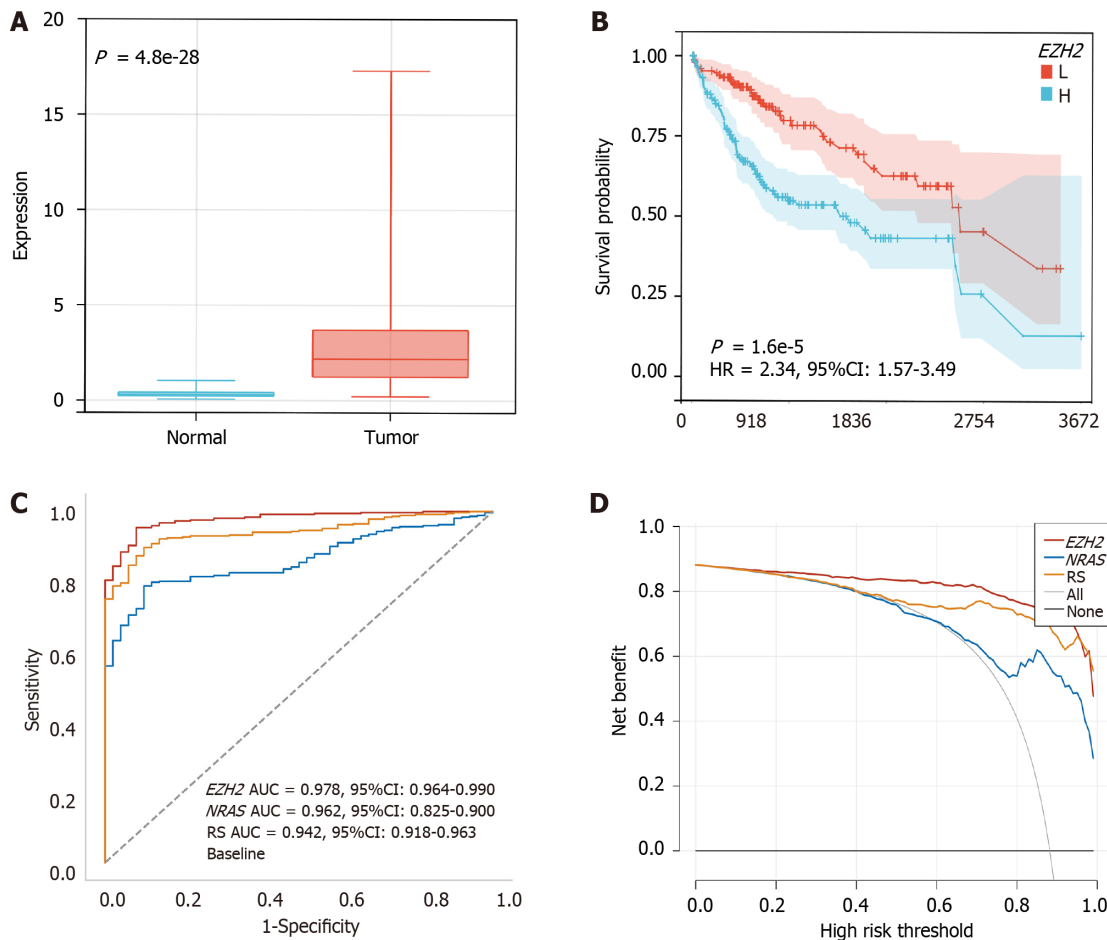


Figure 7 Clinical value of *EZH2* in hepatocellular carcinoma. A: Expression of *EZH2* in hepatocellular carcinoma (HCC) and normal groups; B: High (H) levels of *EZH2* were associated with poor HCC prognosis; C: Receiver operating characteristic curve of *EZH2*, *NRAS*, and risk score (RS) in diagnosing HCC; D: Decision curve analysis of *EZH2*, *NRAS*, and RS in diagnosing HCC. AUC: Area under the curve; CI: Confidence interval; HR: Hazard ratio; L: Low.

LongRunLowGrayLevelEmphasis. Both logistic and random forest algorithms were used to assess feature importance. Notably, original_glrIm-LongRunLowGrayLevelEmphasis and wavelet-LHL_glrIm-LongRunLowGrayLevelEmphasis were closely related to *EZH2* (Figure 8). Based on these findings, we selected original_glrIm-LongRunLowGrayLevelEmphasis and wavelet-LHL_glrIm-LongRunLowGrayLevelEmphasis to construct the *EZH2* prediction-related radiomics model. These steps ensured a comprehensive understanding of the *EZH2* radiomics signature and its potential implications for HCC prediction.

Evaluation of the radiomics model

A comprehensive multimodel analysis was conducted to construct the optimal radiomics model for predicting *EZH2*. The results revealed that the model built using the logistic algorithm not only exhibited better prediction capabilities but also demonstrated greater stability (Table 6 and Figure 9). Consequently, the Radscore was calculated based on the logistic algorithm as follows: Radscore = 0.095 × original_glrIm-LongRunLowGrayLevelEmphasis + 0.671 × wavelet-LHL_glrIm-LongRunLowGrayLevelEmphasis. This approach ensured a robust and accurate prediction of *EZH2* status using radiomics features.

Table 6 Results of predicting EZH2 in the training set and validation set based on the logistic and random forest classifier algorithm

Classification model		AUC	Accuracy	Sensitivity	Specificity	F1 score
Validation	Logistic	0.792	0.667	0.800	0.833	0.833
	Random Forest	0.812	0.750	1.000	0.750	0.833
Training	Logistic	0.787	0.750	0.679	0.881	0.744
	Random Forest	1.000	0.938	1.000	1.000	1.000

AUC: Area under the curve.

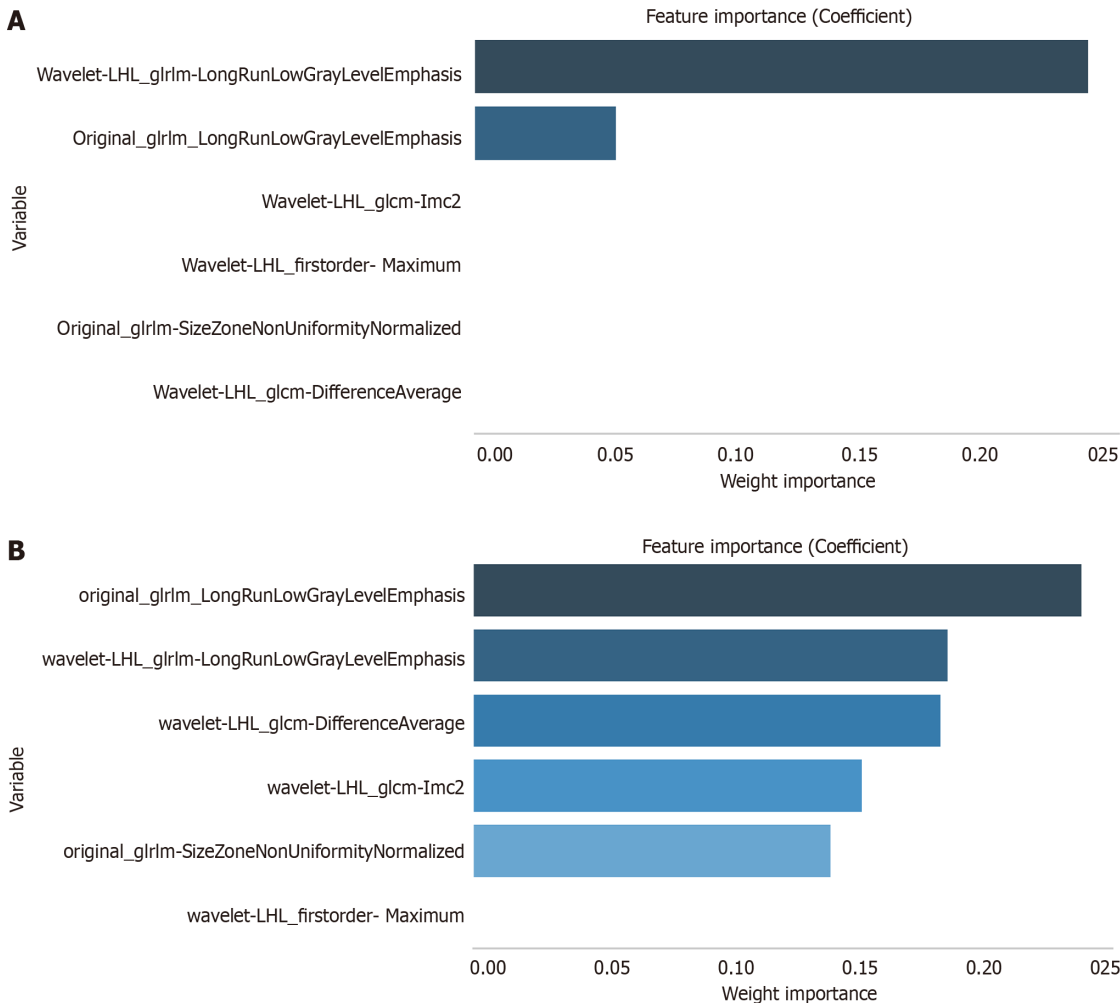


Figure 8 Screening of radiomics features related to EZH2 and radiomics model construction. A: Feature importance based on the logistic algorithm; B: Feature importance based on the random forest algorithm.

Clinical value of the logistic algorithm-radiomics model

The restricted cubic spline revealed a linear relationship between EZH2 and Radscore (Figure 10A). Specifically, the Radscore was higher in the EZH2 high expression group than in the EZH2 low expression group (Figure 10B). Moreover, the Radscore and EZH2 played a crucial role in predicting the OS of HCC patients (Figure 10C). These findings emphasized the significance of EZH2 and its association with patient outcomes in HCC.

DISCUSSION

This study combined radiomics and molecular analyses based on CT images to identify important molecular biomarkers associated with HCC, particularly EZH2. The study also aimed to establish a radiomics model that can predict EZH2 expression and determine its association with HCC prognosis. Consequently, a significant correlation was observed

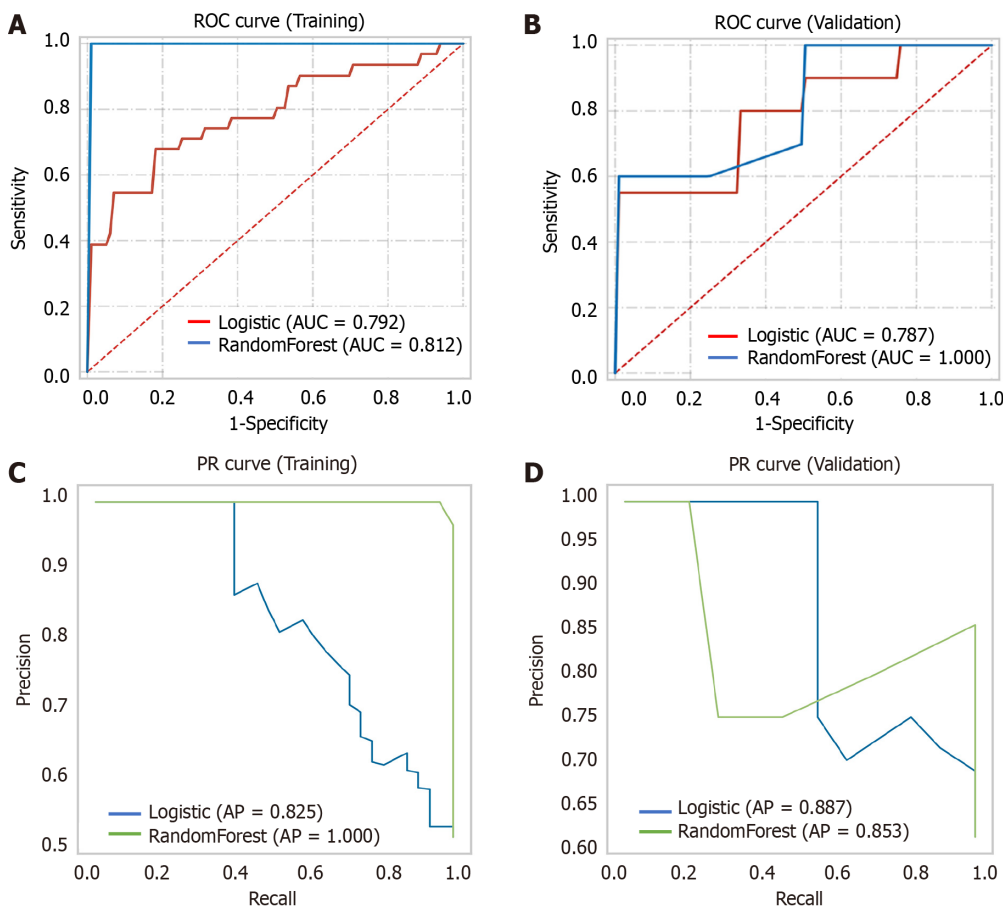


Figure 9 Results of predicting *EZH2* in the training set and validation set based on the logistic and random forest classifier algorithm. A: Receiver operating characteristic (ROC) curve in the training sets based on the logistic and random forest classifier algorithm; B: ROC curve in the validation sets based on the logistic and random forest classifier algorithm; C: Precision (PR) curve in the training sets based on the logistic and random forest classifier algorithm; D: PR curve in the validation sets based on the logistic and random forest classifier algorithm. AP: Average precision; AUC: Area under the curve.

between the radiomics model, *EZH2* expression, and HCC patient prognosis. This finding suggests that radiomics analysis can provide additional molecular information and offer a new approach to the clinical treatment of HCC.

The incidence rate of HCC is increasing globally, and it is generally associated with poor prognosis. Increasing evidence suggests that crosstalk between tumor cells, including HCC, and stromal cells promotes tumor progression[19]. Additionally, CAFs are the predominant stromal cells in the TME of HCC[20]. Liver cirrhosis with a significant number of activated fibroblasts typically predates HCC[21]. Venn diagram analysis identified 299 differentially expressed FRGs in HCC, which are primarily involved in biological processes related to stimuli response pathways including chemical, organic substance, and stress. These pathways are known to participate in tumor development. Through multiple analyses, we established a risk model related to the prognosis of HCC patients composed of two genes, *EZH2* and *NRAS*.

Drug sensitivity analysis revealed a significant negative correlation between *EZH2* and select chemotherapeutic and targeted drugs, while *NRAS* showed no significant correlation. Molecular docking results showed that the *EZH2* (5h14) protein exhibited the strongest binding affinity with the small molecule ligand, belinostat, with a binding energy of -4.58 kcal/mol. In studies with human acute early granulocytic leukemia cells, belinostat independently depleted the histone *EZH2*, leading to the modification of H3 and H4 histones and ultimately achieving therapeutic effects[22]. This suggests that *EZH2* may be a potential therapeutic target for HCC, and belinostat may exert its therapeutic effect by reducing *EZH2* expression levels in HCC.

Further analysis revealed a significant association between *EZH2* expression and poor prognosis in HCC patients. *EZH2* also displayed significant HCC diagnostic capabilities. Therefore, *EZH2* was selected as the primary gene for subsequent analysis. Previous studies have shown that *EZH2* plays an important role in cell lineage determination and related signaling pathways, serving as a major regulator of DNA damage repair, autophagy, cell cycle progression, and cell senescence suppression[23]. The oncogenic mechanism of *EZH2* is primarily by suppressing the expression of tumor suppressor genes in cancer cells[24].

In gliomas, *EZH2* can suppress the differentiation of astrocytes by inhibiting the expression of *BMPR1B*, resulting in increased tumorigenicity in gliomas[25]. *EZH2* also promotes cancer metastasis by silencing E-cadherin and inducing epithelial-mesenchymal transition[26]. In scar research, *RUNX3* mediates the proliferation of fibroblasts by deacetylating *EZH2* through *SIRT1*[27]. In pulmonary fibrosis research, *EZH2* negatively regulates autophagy in the fibrosis through the *lncAPE-ELAVL1* complex[28]. Additionally, CAFs can promote angiogenesis through the VEGF-mediated *EZH2* pathway, and overexpression of *EZH2* is strongly associated with tumor invasion and reduced survival in liver cancer

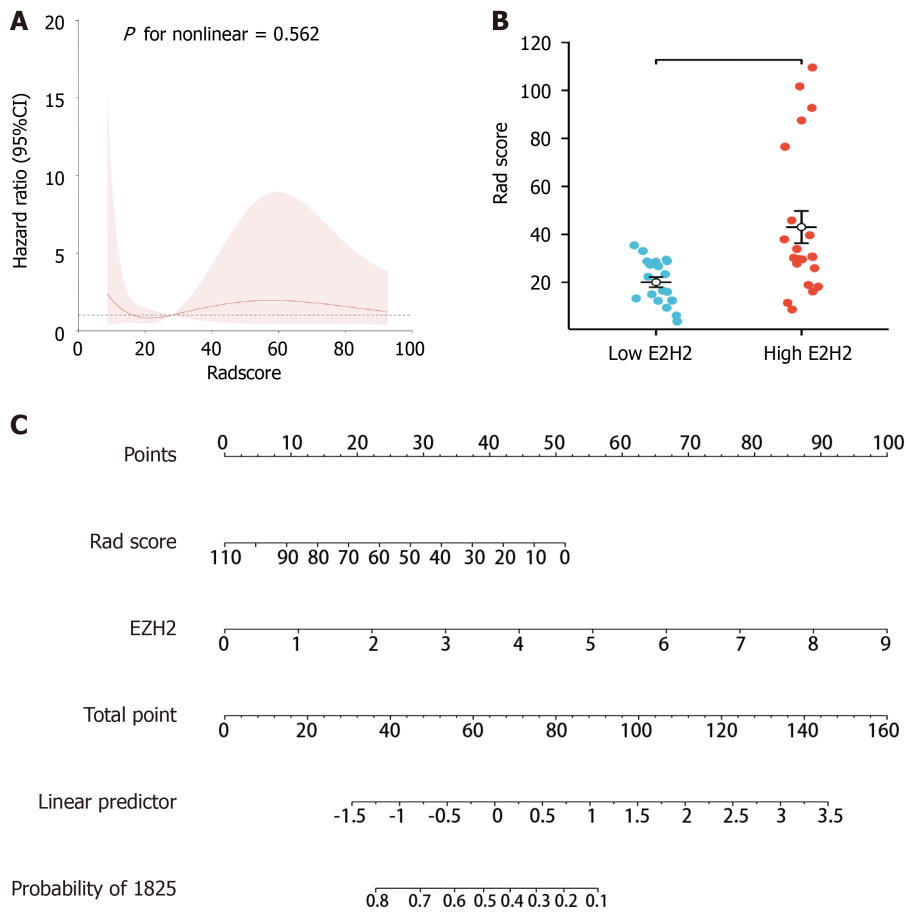


Figure 10 Clinical value of the radiomics model. A: Linear association of *EZH2* and radiomics model; B: Higher Radscore in the high *EZH2* expression group; C: Value of the rad score and *EZH2* in predicting hepatocellular carcinoma prognosis.

patients[29-31]. In conclusion, *EZH2* is not only important for fibroblasts but also plays a significant role in tumor initiation and progression. This is consistent with the results of this study, which found a significant correlation between high *EZH2* expression and poor prognosis in HCC patients.

Radiomics is typically used for diagnosis and postoperative treatment efficacy assessment in HCC[14]. Using the data from preoperative liver-enhanced CT, Feng *et al*[32] constructed a radiomics model to predict the macro trabecular-massive subtype of HCC. Additionally, Xia *et al*[33] were able to predict microvascular invasion in HCC using extracted radiomics features from the preoperative registration or subtraction CT images. This study innovatively linked the radiomics features with *EZH2* expression to use *EZH2* expression to predict the OS of HCC patients from CT image data. A radiomics model related to *EZH2* expression was constructed, and the radiomics features included original_glrIm-LongRunLowGrayLevelEmphasis and wavelet-LHL_glrIm-LongRunLowGrayLevelEmphasis. Gray-Level Run-Length Matrix quantifies gray-level runs, defined as consecutive pixels with the same gray level value[34]. LongRunLowGray-LevelEmphasis is one of the 16 features of Gray-Level Run-Length Matrix, which is a measure of image texture, specifically the roughness. In tendinopathy imaging studies, GLLM-LongRunLowGrayLevelEmphasis can determine tissue changes longitudinally[35]. The higher the value, the rougher the texture. Aside from analyzing the distribution of the gray level of an image, it can also extract representative texture features[31]. In this study, the Radscore was higher in the *EZH2* high expression group, and the radiomics model was efficient in predicting *EZH2* in HCC. The nomogram demonstrated the importance of the Radscore and *EZH2* in predicting the OS of HCC patients. Thus, the radiomics model infers an association with *EZH2* and correlates with the prognosis of HCC patients.

This study leverages advanced imaging and bioinformatics tools to bridge the gap between macroscopic imaging features and microscopic genetic alterations. However, the radiomics and genomics data were obtained from public databases. Additionally, the scarcity of information on the CT images of HCC patients in the TCIA database made it impossible to divide the data into training and validation sets. Lastly, the analytical methods employed in the study primarily consisted of bioinformatics and statistics, lacking relevant experimental validation.

CONCLUSION

In conclusion, the gene model developed in this study, specifically related to fibroblasts in HCC, exhibited a strong association with HCC prognosis. Furthermore, the study identified *EZH2* as a potential therapeutic target linked to the

prognosis of HCC patients. Additionally, a radiomics model associated with *EZH2* can predict *EZH2* expression using CT features, which contributes to the diagnosis and treatment of HCC patients. By combining radiomics with molecular profiling in HCC, this study opens up new avenues for personalized and more effective treatment strategies.

FOOTNOTES

Author contributions: Yu TY and Zhan ZJ contributed to the conception and design; Yu TY, Lin Q, and Huang ZH contributed to the collection and assembly of data; Zhan ZJ and Huang ZH analyzed and interpreted the data; All authors wrote and approved the final manuscript.

Conflict-of-interest statement: There are no conflicts of interest to report.

Open-Access: This article is an open-access article that was selected by an in-house editor and fully peer-reviewed by external reviewers. It is distributed in accordance with the Creative Commons Attribution NonCommercial (CC BY-NC 4.0) license, which permits others to distribute, remix, adapt, build upon this work non-commercially, and license their derivative works on different terms, provided the original work is properly cited and the use is non-commercial. See: <https://creativecommons.org/licenses/by-nc/4.0/>

Country of origin: China

ORCID number: Zhen-Huan Huang 0000-0002-2472-3102.

S-Editor: Fan M

L-Editor: Filipodia

P-Editor: Zhao S

REFERENCES

- 1 Wang T, Dai L, Shen S, Yang Y, Yang M, Yang X, Qiu Y, Wang W. Comprehensive Molecular Analyses of a Macrophage-Related Gene Signature With Regard to Prognosis, Immune Features, and Biomarkers for Immunotherapy in Hepatocellular Carcinoma Based on WGCNA and the LASSO Algorithm. *Front Immunol* 2022; **13**: 843408 [PMID: 35693827 DOI: 10.3389/fimmu.2022.843408]
- 2 Peng X, Zhu J, Liu S, Luo C, Wu X, Liu Z, Li Y, Yuan R. Signature construction and molecular subtype identification based on cuproptosis-related genes to predict the prognosis and immune activity of patients with hepatocellular carcinoma. *Front Immunol* 2022; **13**: 990790 [PMID: 36248822 DOI: 10.3389/fimmu.2022.990790]
- 3 Bray F, Ferlay J, Soerjomataram I, Siegel RL, Torre LA, Jemal A. Global cancer statistics 2018: GLOBOCAN estimates of incidence and mortality worldwide for 36 cancers in 185 countries. *CA Cancer J Clin* 2018; **68**: 394-424 [PMID: 30207593 DOI: 10.3322/caac.21492]
- 4 Liu X, Li J, Wang Q, Bai L, Xing J, Hu X, Li S, Li Q. Analysis on heterogeneity of hepatocellular carcinoma immune cells and a molecular risk model by integration of scRNA-seq and bulk RNA-seq. *Front Immunol* 2022; **13**: 1012303 [PMID: 36311759 DOI: 10.3389/fimmu.2022.1012303]
- 5 Cheng CW, Tse E. Targeting PIN1 as a Therapeutic Approach for Hepatocellular Carcinoma. *Front Cell Dev Biol* 2019; **7**: 369 [PMID: 32010690 DOI: 10.3389/fcell.2019.00369]
- 6 Xu Z, Peng B, Liang Q, Chen X, Cai Y, Zeng S, Gao K, Wang X, Yi Q, Gong Z, Yan Y. Construction of a Ferroptosis-Related Nine-lncRNA Signature for Predicting Prognosis and Immune Response in Hepatocellular Carcinoma. *Front Immunol* 2021; **12**: 719175 [PMID: 34603293 DOI: 10.3389/fimmu.2021.719175]
- 7 Ying F, Chan MSM, Lee TKW. Cancer-Associated Fibroblasts in Hepatocellular Carcinoma and Cholangiocarcinoma. *Cell Mol Gastroenterol Hepatol* 2023; **15**: 985-999 [PMID: 36708970 DOI: 10.1016/j.jcmgh.2023.01.006]
- 8 El-Serag HB. Hepatocellular carcinoma: recent trends in the United States. *Gastroenterology* 2004; **127**: S27-S34 [PMID: 15508094 DOI: 10.1053/j.gastro.2004.09.013]
- 9 Zhang J, Gu C, Song Q, Zhu M, Xu Y, Xiao M, Zheng W. Identifying cancer-associated fibroblasts as emerging targets for hepatocellular carcinoma. *Cell Biosci* 2020; **10**: 127 [PMID: 33292459 DOI: 10.1186/s13578-020-00488-y]
- 10 Loh JJ, Li TW, Zhou L, Wong TL, Liu X, Ma VWS, Lo CM, Man K, Lee TK, Ning W, Tong M, Ma S. FSTL1 Secreted by Activated Fibroblasts Promotes Hepatocellular Carcinoma Metastasis and Stemness. *Cancer Res* 2021; **81**: 5692-5705 [PMID: 34551961 DOI: 10.1158/0008-5472.CAN-20-4226]
- 11 Affo S, Yu LX, Schwabe RF. The Role of Cancer-Associated Fibroblasts and Fibrosis in Liver Cancer. *Annu Rev Pathol* 2017; **12**: 153-186 [PMID: 27959632 DOI: 10.1146/annurev-pathol-052016-100322]
- 12 Kim KH, Roberts CW. Targeting *EZH2* in cancer. *Nat Med* 2016; **22**: 128-134 [PMID: 26845405 DOI: 10.1038/nm.4036]
- 13 Chen S, Pu J, Bai J, Yin Y, Wu K, Wang J, Shuai X, Gao J, Tao K, Wang G, Li H. *EZH2* promotes hepatocellular carcinoma progression through modulating miR-22/galectin-9 axis. *J Exp Clin Cancer Res* 2018; **37**: 3 [PMID: 29316949 DOI: 10.1186/s13046-017-0670-6]
- 14 Xin H, Lai Q, Zhou Y, He J, Song Y, Liao M, Sun J, Li M, Zhang M, Liang W, Bai Y, Zhang Y, Zhou Y. Noninvasive evaluation of neutrophil extracellular traps signature predicts clinical outcomes and immunotherapy response in hepatocellular carcinoma. *Front Immunol* 2023; **14**: 1134521 [PMID: 37520528 DOI: 10.3389/fimmu.2023.1134521]
- 15 Chen M, Cao J, Hu J, Topatana W, Li S, Juengpanich S, Lin J, Tong C, Shen J, Zhang B, Wu J, Pocha C, Kudo M, Amedei A, Trevisani F, Sung PS, Zaydfudim VM, Kanda T, Cai X. Clinical-Radiomic Analysis for Pretreatment Prediction of Objective Response to First Transarterial Chemoembolization in Hepatocellular Carcinoma. *Liver Cancer* 2021; **10**: 38-51 [PMID: 33708638 DOI: 10.1159/000512028]
- 16 Shen Y, Liu J, Zhang L, Dong S, Zhang J, Liu Y, Zhou H, Dong W. Identification of Potential Biomarkers and Survival Analysis for Head and Neck Squamous Cell Carcinoma Using Bioinformatics Strategy: A Study Based on TCGA and GEO Datasets. *Biomed Res Int* 2019; **2019**:

- 7376034 [PMID: 31485443 DOI: 10.1155/2019/7376034]
- 17 **Brenner RJ**, Landgraf AD, Bum-Erdene K, Gonzalez-Gutierrez G, Meroueh SO. Crystal Packing Reveals a Potential Autoinhibited KRAS Dimer Interface and a Strategy for Small-Molecule Inhibition of RAS Signaling. *Biochemistry* 2023; **62**: 3206-3213 [PMID: 37938120 DOI: 10.1021/acs.biochem.3c00378]
 - 18 **Li Q**, Long X, Lin Y, Liang R, Li Y, Ge L. Computed tomography radiomics signature *via* machine learning predicts RRM2 and overall survival in hepatocellular carcinoma. *J Gastrointest Oncol* 2023; **14**: 1462-1477 [PMID: 37435222 DOI: 10.21037/jgo-23-460]
 - 19 **Zhang W**, Huang P. Cancer-stromal interactions: role in cell survival, metabolism and drug sensitivity. *Cancer Biol Ther* 2011; **11**: 150-156 [PMID: 21191189 DOI: 10.4161/cbt.11.2.14623]
 - 20 **Chen S**, Morine Y, Tokuda K, Yamada S, Saito Y, Nishi M, Ikemoto T, Shimada M. Cancer-associated fibroblast-induced M2-polarized macrophages promote hepatocellular carcinoma progression *via* the plasminogen activator inhibitor-1 pathway. *Int J Oncol* 2021; **59** [PMID: 34195849 DOI: 10.3892/ijo.2021.5239]
 - 21 **Tahmasebi Birgani M**, Carloni V. Tumor Microenvironment, a Paradigm in Hepatocellular Carcinoma Progression and Therapy. *Int J Mol Sci* 2017; **18** [PMID: 28216578 DOI: 10.3390/ijms18020405]
 - 22 **Savickiene J**, Treigyte G, Valiuliene G, Stirblyte I, Navakauskiene R. Epigenetic and molecular mechanisms underlying the antileukemic activity of the histone deacetylase inhibitor belinostat in human acute promyelocytic leukemia cells. *Anticancer Drugs* 2014; **25**: 938-949 [PMID: 24800886 DOI: 10.1097/CAD.000000000000122]
 - 23 **Wu SY**, Xie ZY, Yan LY, Liu XF, Zhang Y, Wang DA, Dong J, Sun HT. The correlation of *EZH2* expression with the progression and prognosis of hepatocellular carcinoma. *BMC Immunol* 2022; **23**: 28 [PMID: 35659256 DOI: 10.1186/s12865-022-00502-7]
 - 24 **Han Li C**, Chen Y. Targeting *EZH2* for cancer therapy: progress and perspective. *Curr Protein Pept Sci* 2015; **16**: 559-570 [PMID: 25854924 DOI: 10.2174/1389203716666150409100233]
 - 25 **Lee J**, Son MJ, Woolard K, Donin NM, Li A, Cheng CH, Kotliarova S, Kotliarov Y, Walling J, Ahn S, Kim M, Totonchy M, Cusack T, Ene C, Ma H, Su Q, Zenklusen JC, Zhang W, Maric D, Fine HA. Epigenetic-mediated dysfunction of the bone morphogenetic protein pathway inhibits differentiation of glioblastoma-initiating cells. *Cancer Cell* 2008; **13**: 69-80 [PMID: 18167341 DOI: 10.1016/j.ccr.2007.12.005]
 - 26 **Cao Q**, Yu J, Dhanasekaran SM, Kim JH, Mani RS, Tomlins SA, Mehra R, Laxman B, Cao X, Yu J, Kleer CG, Varambally S, Chinnaiyan AM. Repression of E-cadherin by the polycomb group protein *EZH2* in cancer. *Oncogene* 2008; **27**: 7274-7284 [PMID: 18806826 DOI: 10.1038/onc.2008.333]
 - 27 **Liu H**, Yan G, Li L, Wang D, Wang Y, Jin S, Jin Z, Li L, Zhu L. RUNX3 mediates keloid fibroblast proliferation through deacetylation of *EZH2* by SIRT1. *BMC Mol Cell Biol* 2022; **23**: 52 [PMID: 36476345 DOI: 10.1186/s12860-022-00451-4]
 - 28 **Zhang J**, Wang H, Chen H, Li H, Xu P, Liu B, Zhang Q, Lv C, Song X. ATF3-activated accelerating effect of LINC00941/lncIAPF on fibroblast-to-myofibroblast differentiation by blocking autophagy depending on ELAVL1/HuR in pulmonary fibrosis. *Autophagy* 2022; **18**: 2636-2655 [PMID: 35427207 DOI: 10.1080/15548627.2022.2046448]
 - 29 **Huang B**, Huang M, Li Q. Cancer-Associated Fibroblasts Promote Angiogenesis of Hepatocellular Carcinoma by VEGF-Mediated *EZH2*/VASH1 Pathway. *Technol Cancer Res Treat* 2019; **18**: 1533033819879905 [PMID: 31757187 DOI: 10.1177/1533033819879905]
 - 30 **Zhang L**, Li HT, Shereda R, Lu Q, Weisenberger DJ, O'Connell C, Machida K, An W, Lenz HJ, El-Khoueiry A, Jones PA, Liu M, Liang G. DNMT and *EZH2* inhibitors synergize to activate therapeutic targets in hepatocellular carcinoma. *Cancer Lett* 2022; **548**: 215899 [PMID: 36087682 DOI: 10.1016/j.canlet.2022.215899]
 - 31 **Yang Y**, Zhang Y, Cao J, Su Z, Li F, Zhang P, Zhang B, Liu R, Zhang L, Xie J, Li J, Zhang J, Chen X, Hong A. FGFR4 and *EZH2* inhibitors synergistically induce hepatocellular carcinoma apoptosis *via* repressing YAP signaling. *J Exp Clin Cancer Res* 2023; **42**: 96 [PMID: 37085881 DOI: 10.1186/s13046-023-02659-4]
 - 32 **Feng Z**, Li H, Liu Q, Duan J, Zhou W, Yu X, Chen Q, Liu Z, Wang W, Rong P. CT Radiomics to Predict Macrotrabecular-Massive Subtype and Immune Status in Hepatocellular Carcinoma. *Radiology* 2023; **307**: e221291 [PMID: 36511807 DOI: 10.1148/radiol.221291]
 - 33 **Xia TY**, Zhou ZH, Meng XP, Zha JH, Yu Q, Wang WL, Song Y, Wang YC, Tang TY, Xu J, Zhang T, Long XY, Liang Y, Xiao WB, Ju SH. Predicting Microvascular Invasion in Hepatocellular Carcinoma Using CT-based Radiomics Model. *Radiology* 2023; **307**: e222729 [PMID: 37097141 DOI: 10.1148/radiol.222729]
 - 34 **van Griethuysen JJM**, Fedorov A, Parmar C, Hosny A, Aucoin N, Narayan V, Beets-Tan RGH, Fillion-Robin JC, Pieper S, Aerts HJWL. Computational Radiomics System to Decode the Radiographic Phenotype. *Cancer Res* 2017; **77**: e104-e107 [PMID: 29092951 DOI: 10.1158/0008-5472.CAN-17-0339]
 - 35 **Pintaric K**, Salapura V, Snoj Z, Vovk A, Mijovski MB, Vidmar J. Assessment of short-term effect of platelet-rich plasma treatment of tendinosis using texture analysis of ultrasound images. *Radiol Oncol* 2023; **57**: 465-472 [PMID: 38038412 DOI: 10.2478/raon-2023-0054]



Published by **Baishideng Publishing Group Inc**
7041 Koll Center Parkway, Suite 160, Pleasanton, CA 94566, USA

Telephone: +1-925-3991568

E-mail: office@baishideng.com

Help Desk: <https://www.f6publishing.com/helpdesk>

<https://www.wjgnet.com>

